*PHYSOR 2018: Reactor Physics paving the way towards more efficient systems*
Cancun, Mexico, April 22-26, 2018

# VERIFICATION OF THE INTERACTION PHYSICS OF GUARDYAN A NOVEL GPU-BASED MONTE CARLO CODE FOR SHORT TIME SCALE REACTOR TRANSIENTS

**D. Legrady[1], A. Claret[2], B. Molnar[1], G. Tolnai[1]**

[1]Budapest University of Technology and Economics
Budapest, Muegyetem rkp. 3, H-1111, Hungary, Europe

[2] Student at Ecole Nationale Supérieure d'Arts et Métiers F PARIS062
151 boulevard de l'Hôpital 75013 Paris, France, Europe

legrady@reak.bme.hu, amaury.claret@orange.fr, molba@reak.bme.hu, tolnai@reak.bme.hu

## ABSTRACT

The novel GPU assisted Monte Carlo code GUARDYAN targeting applications of reactor transient analysis has been compared to simulations of MCNP for verification purposes. In 2000 separate calculations using 412 isotopes, about 445 000 data points were generated and compared with MCNP6. Results showed agreement within statistics.

KEYWORDS: GPU, Monte Carlo, Reactor Dynamics, Verification, Neutronics

## 1. INTRODUCTION

GUARDYAN (GpU Assisted Reactor DYnamic ANalysis) [1] developed at Budapest University of Technology and Economics is a novel Monte Carlo based neutron transport code running on GPU (Graphics Processing Unit) targeting applications of reactor transients with timescale in the order of seconds. This paper summarizes the code verificaion efforts consisting of comparisons of calculation results to the code MCNP6 [2]. The GUARDYAN code flow is based on simulating consecutive time intervals rather than following neutron generations from fission to fission, facilitating fast reactor transient simulations as proposed and developed in [3,4]. The code GUARDYAN harnesses the power of GPUs to fulfill the computing needs. Investigation of two different GPU implementation strategies of the Monte Carlo method using GUARDYAN is presented in [5].

At the current development stage full handling of neutron interaction physics is included based on ENDF-B-VII.1 data except for S($\alpha$,$\beta$) treatment and unresolved resonances. Interaction sampling is similar to the methods applied in MCNP and OpenMC [6]. Geometry handling is also similar in concept and in sophistication to MCNP, OpenMC and SERPENT [7]. Source definition and tally setup however is focusing on reactor models regarding mostly power evolution and distribution estimation and coupling to thermohydraulics, all being currently at the early stages of development.

This paper focuses on the verification of the interaction physics of GUARDYAN. A simple spherical geometry was set up and the outgoing particles on the bounding sphere were counted in 24 logarithmic energy and 9 linearly spaced time bins for 5 starting energies by both MCNP6 and GUARDYAN using

the same cross section tables. Separate calculations were carried out for the most relevant 412 isotopes where sphere sizes were individually chosen to yield meaningful tallies. In total some 445 000 data points were compared. Further a small subcritical model was put together in a water sphere with uranium cylinders. Discrepancies were within statistics even when rarer interactions were more probably sampled.

This paper is organized as follows: first we show a brief introduction of GUARDYAN including motivation for the development, features list and most importantly interaction physics. Next we show the comparison methodology and we analyze the results.

## 2. GUARDYAN FEATURES

### 2.1. Motivation

On a worldwide scale efforts targeted at Monte Carlo based reactordynamics codes are about to leave scouting phase and turn towards bringing proof-of-concept schemes closer to realistic industrial applications [8]. The development of GUARDYAN approaches this topic by focusing on massively parallel architectures such as General Purpose GPU's. Recently commercially available GPU memory sizes reached 8 Gbyte breaking through the barriers associated with memory needs of an industrial application. For reference, a fully detailed geometry and cross section model of a commercial VVER-440 power plant geometry was created in GUARDYAN necessitating 5 Gbyte of memory including cross sections preprocessed for fast Monte Carlo sampling. Hardware developers recently announced GPU memory capacities of 24 Gbyte and up, finally clearing all the obstacles standing in the way of industrial size applications. GPU implementation is expected to offer at least a factor 5 speedup compared to similarly priced CPU's (Central Processing Unit) if the GPU calculation flow is optimized to use the hardware capacities. This latter condition is not to be overlooked: a poorly demised parallelization scheme can very easily underperform the CPU implementations of decades of careful optimization work.

Implementation of GUARDYAN started in 2015 in the frame of VKSZ_14-1-2015-0021 Hungarian project supported by the (Hungarian) National Research, Development and Innovation Fund. The code is expected to include full physics modeling capabilities, kinetic calculation capabilities without thermal feedback and rudimentary thermohydraulic modeling with feedback at the project end of 2019.

### 2.2. Calculation Flow and Variance Reduction

Vectorization of a MC code addresses the issue of what is called thread divergence in GPU terminology (different tasks are assigned to working units, resulting in the degradation of parallel performance). At the beginning of the development of General Purpose GPU's collections of threads called *warps* were set to perform the same calculation on multiple data sets. If a thread in a warp takes longer to calculate the other threads are stalled and calculation efficiency degrades. If Monte Carlo simulations follow nuclear particles especially if neutron transport is considered, one history may be significantly longer than the other, thus threads diverge. Current GPU architectures are less strict on this rule and optimize workload very efficiently, still GUARDYAN aims at creating equal workload for each history by eliminating history branching and minimizing particle loss. Fission is therefore treated with weight change, similarly implicit capture is applied instead of loss to capture.

In practice another feature of GPU's limited the efficiency of the code more than thread divergence: register use. GPU's are low in operative memory and threads may compete for memory resources. In our practice careless register use may very easily keeps the GPU workload below 50%.

Instead of a quasistatic neutronics simulation with estimation of parameters like $k_{eff}$, in each time step GUARDYAN simulates the time evolution of fission chains thereby the length of the histories (number of interactions before the end of the given time interval) can be kept similar. The neutrons are followed from the beginning to the end of a time interval. Particle capture is taken care of implicitly with weight reduction. Fission is also taken care of as weight increase. In a fissionable material interaction probability is biased, with total fission cross section without absorption $\Sigma_f$, total cross section $\Sigma_t$ and scattering cross section $\Sigma_s$, a fission event is selected with probability $(\Sigma_t - \Sigma_s)/\Sigma_t$ and weigh becomes $\nu\Sigma_t/(\Sigma_t - \Sigma_s)\Sigma_f$ with $\nu$ total fission yield. Further variance reduction techniques are under development [9]. At the end of each time step the neutron (both prompt and precursor) population is reorganized (population combing, like in [10]) to replace loss due to escape by splitting high weight particles. This algorithm structure ensures that in each calculation step a constant neutron population samples the reactor geometry. As a further consequence GUARDYAN is not optimized for $k_{eff}$ calculations and such feature is only present for code intercomparison purposes. In future code releases dynamic $k_{eff}$ (as discussed in [11]) estimation is planned as .

### 2.3. Geometry Handling

Similarly to other Monte Carlo particle transport codes (Serpent, MCNP, OpenMC) in GUARDYAN geometry is defined by cells with homogenous material composition. Cells are defined by Boolean operators of bounding surfaces. These data can be given in *xml* files in a format closely following the input logic of Serpent, MCNP and OpenMC. Fig. 1 contains the list of available surfaces and as an illustration a cross section view of the Hoogenboom-Martin benchmark geometry [12]

| | |
|---|---|
| $px$ | $x - x_0$ |
| $py$ | $y - y_0$ |
| $pz$ | $z - z_0$ |
| $p$ | $Ax + By + Cz - D$ |
| $cx$ | $y^2 + z^2 - r^2$ |
| $cy$ | $x^2 + z^2 - r^2$ |
| $cz$ | $x^2 + y^2 - r^2$ |
| $c/x$ | $(y - y_0)^2 + (z - z_0)^2 - r^2$ |
| $c/y$ | $(x - x_0)^2 + (z - z_0)^2 - r^2$ |
| $c/z$ | $(x - x_0)^2 + (y - y_0)^2 - r^2$ |
| $so$ | $x^2 + y^2 + z^2 - r^2$ |
| $sx$ | $(x - x_0)^2 + y^2 + z^2 - r^2$ |
| $sy$ | $x^2 + (y - y_0)^2 + z^2 - r^2$ |
| $sz$ | $x^2 + y^2 + (z - z_0)^2 - r^2$ |
| $s$ | $(x - x_0)^2 + (y - y_0)^2 + (z - z_0)^2 - r^2$ |
| $sq$ | $A(x-x_0)^2+B(y-y_0)^2+C(z-z_0)^2+2D(x-x_0)+2E(y-y_0)+2F(z-z_0)+G$ |
| $kx$ | $\sqrt{y^2 + z^2} - t(x - x_0)$ |
| $ky$ | $\sqrt{x^2 + z^2} - t(y - y_0)$ |
| $kz$ | $\sqrt{x^2 + y^2} - t(z - z_0)$ |
| $k/x$ | $\sqrt{(y - y_0)^2 + (z - z_0)^2} - t(x - x_0)$ |
| $k/y$ | $\sqrt{(x - x_0)^2 + (z - z_0)^2} - t(y - y_0)$ |
| $k/z$ | $\sqrt{(x - x_0)^2 + (y - y_0)^2} - t(z - z_0)$ |
| $tx$ | $\frac{(x-x_0)^2}{B^2} + \frac{\left(\sqrt{(y-y_0)^2+(z-z_0)^2}-A\right)^2}{C^2} - 1$ |
| $ty$ | $\frac{(y-y_0)^2}{B^2} + \frac{\left(\sqrt{(x-x_0)^2+(z-z_0)^2}-A\right)^2}{C^2} - 1$ |
| $tz$ | $\frac{(z-z_0)^2}{B^2} + \frac{\left(\sqrt{(x-x_0)^2+(y-y_0)^2}-A\right)^2}{C^2} - 1$ |

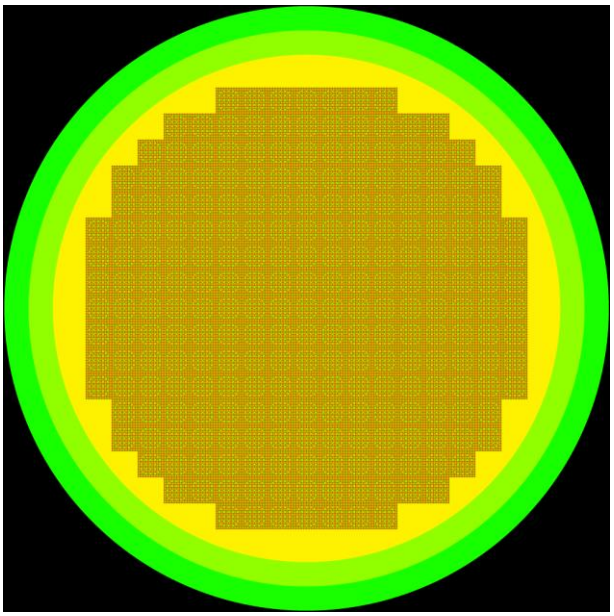

**Figure 1. List of available bounding surfaces (left) and a cross section of the Hoogenboom-Martin benchmark geometry**

Cells may be filled into either rectangular or hexagonal lattices. Surfaces can be transformed by arbitrary rotation matrices. Geometry input is optimized for later use in cell lookup at free path sampling.

For a further illustration of geometry descriptor features, the core of the Training Reactor of the Budapest University of Technology and Economics was modeled and some neutron transport steps were carried out. Fig. 2 left-hand-side shows the geometry map of the core at a certain cross section with lighter blue

circles showing the position of the fuel rods, darker blue tiles are reflectors; black, orange and yellow circles show control and safety rods or other absorbers; green indicates water.

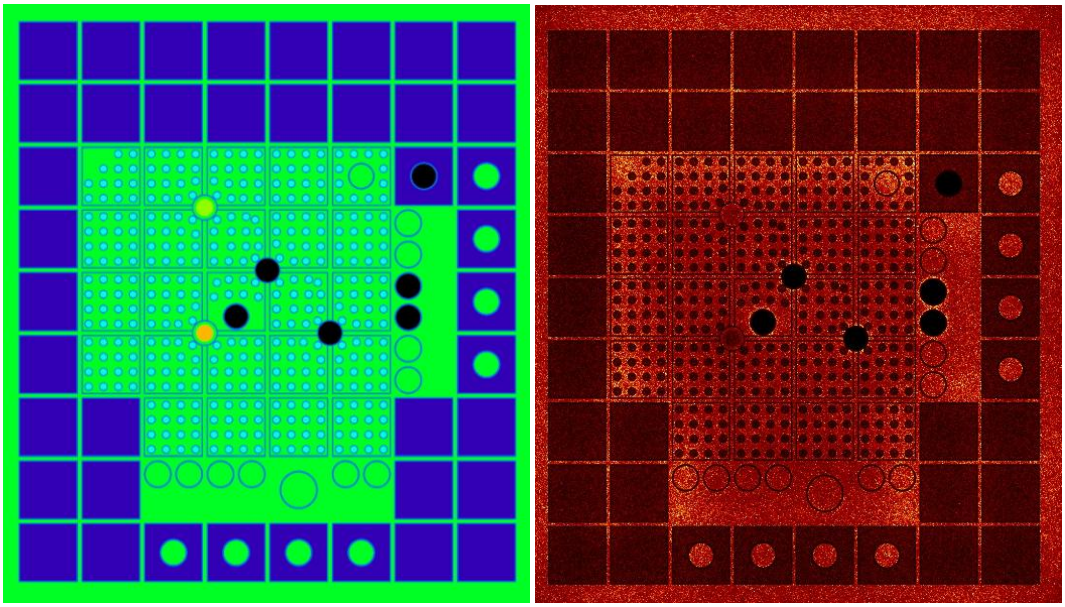

**Figure 2. Budapest Training Reactor geometry (left) and neutron density at a certain time instance (right), lighter shades indicate higher neutron density**

In the right-hand-side of Fig. 2 neutron density is calculated at a certain time instance with 6 $10^7$ neutrons used for the image. The geometry consists of 42 isotopes, 66 surfaces, 84 cells, 13 lattices and 11 universes.

Time dependent cross section changes can currently be given as subsequent geometry input files belonging to different time steps. User friendliness in this regard would be increased in later code versions .

### 2.4. Interaction Sampling

GUARDYAN uses the cross section data table *ENDF/B-VII.1* [13] in ACE (*A Compact ENDF*) format. Interaction sampling follows similar techniques as in MCNP and OpenMC. Albeit not optimal for GPU applications, we have chosen the already paved way in order to create an easily verifiable code. Major efficiency gain is expected from transforming interaction sampling towards eliminating rejection steps even in exchange for particle weight change: the latter being disadvantageous for the statistical variance the former minimizing thread divergence. A more GPU targeted sampling schematic is planned for future code versions after the full physics modeling is present and verified using the more conventional interaction sampling algorithms.

Free path sampling follows the Woodcock (delta-tracking) scheme with energy dependent majorant sampling cross section. The selection of isotope and interaction type happens in the analog way except for choosing between scattering and fission events.

We consider reactions with the following MT numbers: 2, 5, 11, 16, 17, 18, 19, 20, 21, 22, 23, 24, 25, 28, 29, 30, 32, 33, 34, 35, 36, 37, 38, 41, 44, 45, 51-90, 101. After choosing the reaction, the determination of the new energy and angle of the neutron depends on the given ACE law (ACE Laws 3, 4, 7, 9, 11, 44, 61

or 66 ). $S(\alpha,\beta)$ treatment and handling unresolved resonances are not yet included in the physics modeling.

## 3. VERIFICATION

### 3.1. Verification Parameter Set

Often a verification of a newly implemented reactor physics code is done in an integral sense, on a near critical assembly with complicated geometry and the estimation of integral parameters like the $k_{eff}$ is compared to a well established code calculation result. As GUARDYAN is meant primarily to simulate time evolution of power level and flux we have decided to compare time and energy spectra separately for a broad selection of isotopes. A small *subcritical model* was also created for validating geometry features and isotope mixture handling.

The verification *basic model* was a sphere containing a single isotope with density belonging to the natural isotope abundance. Neutrons were started at time zero. In separate calculations 5 starting energies were selected: $10^{-8}$, $10^{-6}$, $10^{-3}$, 1, 18MeV thereby the interaction types for the full relevant energy range (from thermal up to the energy limit of commonly available cross section data). For each isotope the radius of the sphere was set to three times the free path length at the neutron starting energy. First GUARDYAN was executed and the particles registered at the outer bounding surface of the sphere. Next, using smallest and largest values of energy and time of the Guardyan samples a tally bin structure is set up with 24 logarithmic energy bins and 9 equally spaced time bins. MCNP6 input was generated and executed with these tally settings.

The list of isotopes includes every isotope present in *ENDF/B-VII.1*, except for the metastable ones.

The *subcritical model* was a 30cm radius water sphere with 61 $UO_2$ cylindrical fuel rods of 40cm length, 1cm radius spaced 1cm apart from each other as illustrated by Fig.3. Uranium was 4.7% enriched and fuel rod density was taken as 10.5g/cm$^3$.

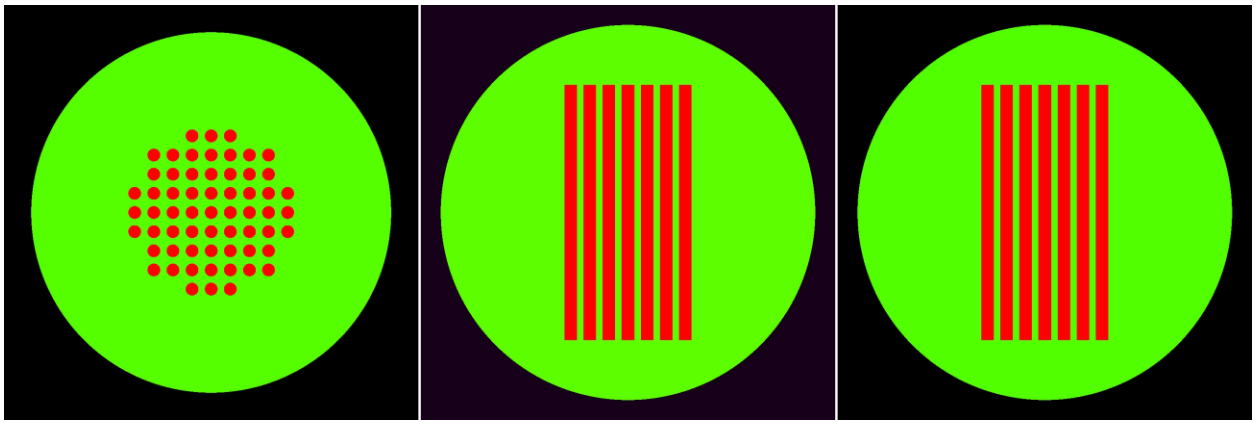

**Figure 3. Subcritical model geometry: $UO_2$ rods in a water sphere cross sections perpendicular to z,x and y axes' from left to right respectively**

Similarly, a time-energy spectrum is registered in this case as well.

### 3.2. Verification Results

#### 3.2.1. Results for the basic model

For each isotope a figure has been created for visual inspection such as in Fig. 4. Separate figures are energy spectra of the number of particles crossing the sphere outer surface divided by the starting particle number. Each subfigure belongs to a separate time interval. Additional information is also gathered like the running time of the calculation (note that MCNP was run on a single processor), number of points with discrepancies between MCNP and GUARDYAN falling below 1%, number of nonzero estimates (where $\sigma$ the error estimate is above zero), etc.

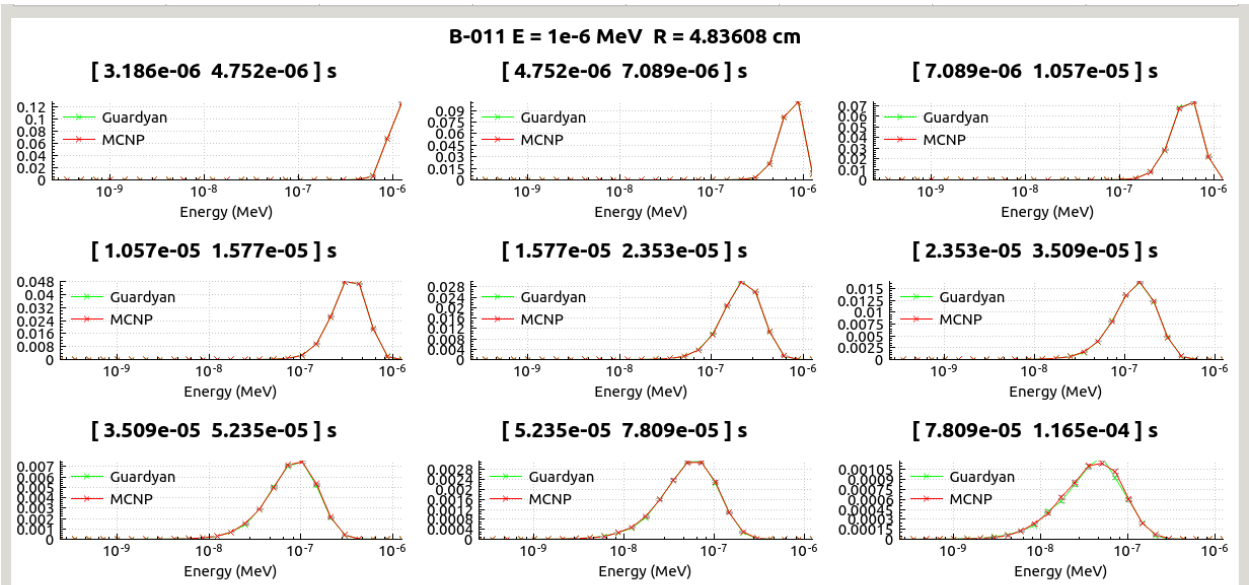


| MCNP elapsed time | Guardyan elapsed time | Δ < 1.0 % | σ > 0.0 % | x^2 | < 1 σ | < 2 σ | < 3 σ |
|---|---|---|---|---|---|---|---|
| 10261 ms | 638 ms | 41 | 131 | 0.995585 | 67.1756% | 95.4198% | 100% |

**Figure 4. Basic model results comparison for $^{11}$Be, $10^{-6}$ MeV**

With careful inspection each of these figures were analyzed and if discrepancies were found the origins were identified and if it was a programming error, it was fixed.

As a result a total of some 445 000 data points were compared at the final stage. A reduced $\chi^2$-like statistics was calculated as:

$$\chi^2 = \frac{1}{N}\sum_{i=1}^{N}\frac{\left(y_{M,i}-y_{G,i}\right)^2}{\sigma_{M,i}^2+\sigma_{G,i}^2}, \quad (1)$$

where $N$ is the number of $i$ data points for a single isotope a single starting energy (i.e. N= 9x 24 = 216 ), σ stands for the standard deviation of the Monte Carlo estimates (M for MCNP, G for GUARDYAN) and $y$ is the tally results. It means that squared difference is compared against the sum of squared standard deviations, thus $\chi^2$ should be below 1 is if the results fall within 1 standard deviation, in most cases it should be below 2 and results above 3 should be rare.

As for the all of the cases discrepancies of the results were rarely detectable while relative errors were only a few percent we have decided to further analyzes the results and summarize the results in terms of $\chi^2$. With each $\chi^2$ calculated, we obtain 412 isotopes times 5 energies. These results are displayed in Fig.5.

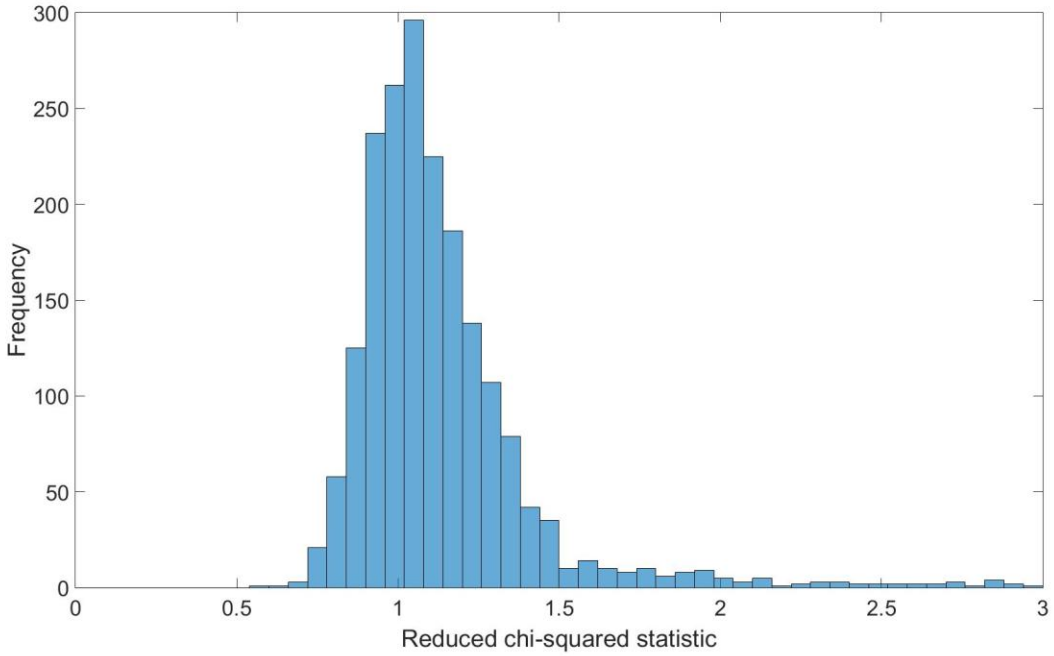


**Figure 5. Histogram of $\chi^2$values**

As Fig. 5 shows GUARDYAN and MCNP results agree very well within statistics having the majority of the cases with match within 1.5σ. Given that the statistical errors were in the range of 1%-5% the remaining discrepancies must be very small in magnitude.

For lower energies, in vast majority of the isotopes the dominant interaction is elastic scattering. For fissionable materials ACE laws 3, 4, 7, 9, 11, 44, 61 and 66 occur even at low energies, for higher energies many isotopes undergo such interactions, still elastic scattering being the dominant interaction in case of the basic model. To ensure that promising $\chi^2$ values are not only caused by a properly implemented elastic scattering algorithm, we have registered the number of samplings of certain ACE laws. To assess the impact of a certain ACE law on the $\chi^2$ value we have calculated the (Pearson) correlation coefficient between $x_i$ and $y_i$ data points with $\bar{x}$ and $\bar{y}$ averages respectively:

$$corr = \frac{\sum_{i=1}^{n}(x_i-\bar{x})(y_i-\bar{y})}{\sqrt{\sum_{i=1}^{n}(x_i-\bar{x})^2}\sqrt{\sum_{i=1}^{n}(y_i-\bar{y})^2}}, \quad (2)$$

.

Table I. shows the correlation of the number of a certain ACE law sampling with the $\chi^2$ values for different neutron starting energies. Near zero correlation coefficients indicate no correlation, near 1 or -1 strong linear correlation.

Elastic scattering appears always with near zero coefficients with consistently negative sign. At $10^{-8}$ MeV and 18MeV the correlation is greater but still negative; we may interpret this as elastic scattering contributing to better match of results. ACE Law 3 (inelastic level scattering), ACE Law 4 (continuous tabular distribution) and ACE Law 61 (correlated energy and angle distribution) show a clearly nonzero

and often positive correlation indicating that the GPU implementation differ from MCNP. All three of these sampling processes happen with high energy neutrons, for low starting neutron energies the interactions happen after fission has occurred. Number of sampled interactions with these laws shows that without fissile material present, none of these sampling processes are called.

**Table I. Correlation Coefficients of $\chi^2$ values with number of interactions sampled by a certain ACE law**

| | $10^{-8}$ MeV | $10^{-6}$ MeV | $10^{-3}$ MeV | 1MeV | 18Mev |
|---|---|---|---|---|---|
| Elastic scattering | -0.21372 | -0.01053 | -0.05259 | -0.07189 | -0.26171 |
| ACE Law 3 | 0.4743 | 0.43175 | 0.41582 | -0.05454 | -0.15467 |
| ACE Law 4 | 0.30463 | 0.32031 | 0.67385 | 0.45868 | 0.17577 |
| ACE Law 7 | -0.00399 | -0.00405 | 0.01045 | -0.00808 | -0.00166 |
| ACE Law 9 | -0.00872 | -0.00649 | 0.01524 | -0.00716 | 0.03139 |
| ACE Law 11 | -0.01198 | 0.00382 | 0.05435 | 0.00464 | 0.00769 |
| ACE law 44 | 0.00206 | -0.00254 | 0.04434 | 0.14184 | -0.03327 |
| law61 | 0.31364 | 0.21316 | 0.50553 | -0.00556 | -0.09562 |
| law66 | -- | -- | -- | -- | -0.00607 |

ACE Law 3 and 61 for higher starting neutron energies show almost zero correlation coefficient, i.e. at energies where the ratio of sampling number to elastic scattering is the highest, yielding the conclusion that the these law sampling schemes are not suspicious. For fissile materials the simulation chain lengths vary with number of collisions in a chain following geometrical distribution yielding a less robust estimation. ACE Law 4 shows the same behavior but higher energies still show higher correlation coefficients while this sampling process is very often called for most of the isotopes. Further research will target the solution of this issue.

### 3.2.2. Results for the subcritical model

Results for the subcritical model is shown in Fig. 6.

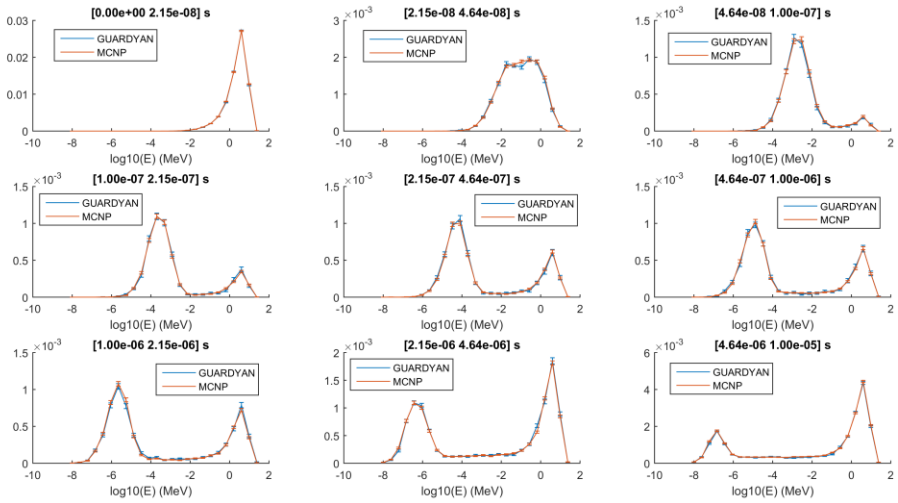


**Figure 6. Fluence spectra for the subcritical model**

Neutrons were started again in the middle of the geometry, with 10MeV starting energy. In the first three time intervals the neutrons thermalize and from the fourth time step on fission neutrons start to appear, and for the last time step the fission neutrons dominate the spectrum again. For this process neutrons had to transverse geometry, select interaction, slow down by scattering reactions, captured by absorption and finally escape or induce fission. As Fig. 6 shows every important reaction for a reactor neutronics is sampled and the previously shown isotope-by-isotope verification process also matches MCNP results for a –though very simplified, but still a -.reactor application.

## 4. CONCLUSIONS

GUARDYAN verification efforts consisted of running some 2000 geometries with both MCNP6 and GUARDYAN generating about 445 000 data points to compare. Results match within statistics. Correlation analysis according to ACE Laws showed a minor discrepancy at ACE Law 4 that indicates systematical deviation from the MCNP results, but still within the range of statistics. This discrepancy should further be analyzed with dedicated simulations restricted to relevant MT numbers and energies.

Future work should further consist of including the treatment of unresolved resonances and S($\alpha$,$\beta$).

## ACKNOWLEDGMENTS

This work has been carried out in the frame of VKSZ_14-1-2015-0021 Hungarian project supported by the National Research, Development and Innovation Fund.

## REFERENCES

1. http://awing.reak.bme.hu/GUARDYAN
2. T. Goorley, et al., "Initial MCNP6 Release Overview", *Nuclear Technology*, **180,** pp 298-315 (Dec 2012)
3. B. L. Sjenitzer, J. E. Hoogenboom, „Dynamic Monte Carlo Method for Nuclear Reactor Kinetics Calculations", *Nuclear Science and Engineering* , **175** (1) / pp. 94-107.
4. D. Legrady, J E: Hoogenboom, "Scouting the Feasibility of Monte Carlo Reactor Dynamics Simulations", *Proceedings of International Conference on the Physics of Nuclear Reactors*, Interlaken, Switzerland, 2009
5. B. Molnar, G. Tolnai, D. Legrady, M. Szieberth, „Vectorized Monte Carlo for Guardyan – A, GPU accelerated Reactor Dynamics Code", *This Conference*
6. https://openmc.readthedocs.io/en/stable/
7. J. Leppänen, et al. (2015) "The Serpent Monte Carlo code: Status, development and applications in 2013*"." Ann. Nucl. Energy*, 82 pp 142-150. (2015),
8. http://cordis.europa.eu/project/rcn/211032_en.html
9. D. Legrady, B. Molnar, M. Klausz, and T. Major. "Woodcock tracking with arbitrary sampling cross section using negative weights." *Annals of Nuclear Energy*, volume 102, pp. 116–123 (2017).
10. T. E. Booth. "A weight (charge) conserving importance-weighted comb forMonte Carlo". In *Proceedings of Radiation Protection and Shielding Division TopicalMeeting*. N. Falmouth, MA, 1996
11. D. E. Cullen, C. J. Clouse, R. Procassini, and R. C. Little, "Static and dynamic criticality: are they different?" Report UCRL-TR-201506, Lawrence Livermore National Laboratory, Livermore, California, USA, 2003.
12. J. E. Hoogenboom and W. R.Martin. "A proposal for a benchmark to monitor the performance of detailed Monte Carlo calculation of power densities in a full size reactor core". In *Proceedings of American Nuclear Society - International Conference on Mathematics, Computational Methods and Reactor Physics 2009,M&C2009*, 2009.

13. M.B. Chadwick, et. al "ENDF/B-VII.1: Nuclear Data for Science and Technology: Cross Sections, Covariances, Fission Product Yields and Decay Data", *Nucl. Data Sheets* **112**(2011)2887.